Force-Clamp Spectroscopy of Single-Protein Monomers Reveals the Individual Unfolding and Folding Pathways of I27 and Ubiquitin

Sergi Garcia-Manyes, Jasna Brujić, Carmen L. Badilla, and Julio M. Fernández
Department of Biological Sciences, Columbia University, New York, New York, 10027

ABSTRACT Single-protein force experiments have relied on a molecular fingerprint based on tethering multiple single-protein domains in a polyprotein chain. However, correlations between these domains remain an issue in interpreting force spectroscopy data, particularly during protein folding. Here we first show that force-clamp spectroscopy is a sensitive technique that provides a molecular fingerprint based on the unfolding step size of four single-monomer proteins. We then measure the force-dependent unfolding rate kinetics of ubiquitin and I27 monomers and find a good agreement with the data obtained for the respective polyproteins over a wide range of forces, in support of the Markovian hypothesis. Moreover, with a large statistical ensemble at a single force, we show that ubiquitin monomers also exhibit a broad distribution of unfolding times as a signature of disorder in the folded protein landscape. Furthermore, we readily capture the folding trajectories of monomers that exhibit the same stages in folding observed for polyproteins, thus eliminating the possibility of entropic masking by other unfolded modules in the chain or domain-domain interactions. On average, the time to reach the I27 folded length increases with increasing quenching force at a rate similar to that of the polyproteins. Force-clamp spectroscopy at the single-monomer level reproduces the kinetics of unfolding and refolding measured using polyproteins, which proves that there is no mechanical effect of tethering proteins to one another in the case of ubiquitin and I27.

INTRODUCTION

Force spectroscopy using atomic force microscopy (AFM) has proven to be a primary tool in revealing a wealth of new information regarding the mechanical unfolding and refolding properties of a wide variety of multidomain proteins under a pulling force. So far, single-molecule mechanical experiments have been conducted using either engineered tandem identical repeats of a single protein module (1) or double-cysteine polymerization (2,3) to ensure a fingerprint for the unfolding of the single molecule under investigation. In either case, the use of concatamers can unambiguously distinguish between the nonspecific adhesion interactions of the cantilever and the surface and the length trajectories resulting from stretching the polyprotein (4). However, the effect of tethering multiple protein domains in a chain on the (un)folding process has been a subject of much debate in biology, suggesting domain-domain interactions (5–9), aggregation (10–12), domain swapping (13), or energy storage through the molecular spring (14). Directly related to our experiments, the folding trajectories of multiple domains monitored by the force-clamp technique have been challenged by the protein-folding community as being attributable to either aggregation (12) or entropic masking in the spring (15). Although previous studies have employed the use of uncharacterized monomer proteins bracketed by chimera I27 (16–18) or GB1 handles (19) to probe the mechanical unfolding pathways by force extension, this approach still encounters the same issues because multiple proteins are present in the chain. Even though many modular proteins are naturally found to perform their function in tandem (20–25), the majority of proteins perform their biological function in their monomeric form, deserving particular attention.

Here we introduce a new single-monomer approach in force-clamp spectroscopy, which allows for the investigation of the kinetics of unfolding as well as the subsequent refolding of individual protein modules. The only other experiment with such a capability probes the low-force regime using laser tweezers on RNase H, which employs a complex setup involving DNA molecular handles (26). Here we avoid the use of such handles, which sets the stage for the observation of the folding process along the well-defined length reaction coordinate over time. The compromise in using monomers is the lack of a definitive fingerprint based on the unfolding step size, as there is no repeating pattern characteristic of polyproteins. Even so, the prevalence of data with the expected step size allows for a thorough investigation. In what follows, we present a control experiment using monomers to resolve a number of controversies encountered by the polyprotein force-clamp data.

As the name suggests, force-clamp spectroscopy employs an electronic feedback system with a 3-ms time resolution to hold a single molecule at a constant pulling force over time. In the case of a polyprotein, the resulting length-versus-time traces (27) exhibit staircases in which the height of every step serves as a fingerprint for the unfolding of each particular module and marks the unfolding dwell time, t, from the moment the force is applied. An average of a few such unfolding traces therefore gives the probability of unfolding as a function of time, which can be approximated by an average unfolding rate for each stretching force. We have

Submitted January 16, 2007, and accepted for publication April 25, 2007.

Address reprint requests to J. M. Fernández, Department of Biological Sciences, Columbia University, New York, NY, 10027. E-mail: jfernandez@columbia.edu.

Editor: Stuart M. Lindsay.

0006-3495/07/10/2436/11 $2.00

doi: 10.1529/biophysj.107.104422

shown that polyubiquitin unfolding as a function of force can be approximated by the simple Bell model (28,29).

Another important aspect of polyprotein unfolding is the influence of the number of modules in the polyprotein chain, N, on the unfolding process. Because the cantilever picks up chains from random positions on the surface, N varies from one module up to the engineered protein length. However, molecules often detach from the cantilever before all the modules have unfolded, which introduces an uncertainty in N. Nevertheless, using trajectories that do not detach for a minimum of 4 s, we have recently found that the average rate of unfolding is independent of N, suggesting that the modules unfold independently of one another (30). If this Markovian hypothesis holds true, the monomer proteins should give rise to the same unfolding rates as their polyprotein counterparts. Indeed, we find that the monomers obey the same trends as the polyproteins as a function of the stretching force, reproducing the same distances to the unfolding transition states in ubiquitin and I27.

Furthermore, recent experiments on an extensive pool of unfolding data have shown important deviations from two-state kinetics in ubiquitin at a constant force of 110 pN (31). In this unfolding dwell time analysis at the chain level, we employed the binomial distribution, according to which the dwell times depend on both the variations in N and the order number of the event in the chain. The maximum-likelihood method (MLM) was then used to allocate a rate of unfolding and N to each trajectory. This method implicitly accounts for the fact that molecules can detach before all the modules have unfolded, but the heterogeneity in the rates cannot be decoupled from the uncertainty in N. Moreover, the obtained distribution is narrowed down by the averaging inherent to the technique, such that we used Monte Carlo simulations to predict the real distribution of rates explored at the monomer level. This kinetic analysis uncovered power-law-distributed unfolding rates spanning more than two decades, which are suggestive of a complex energy landscape with multiple energy minima or traps. In the trap model (32), this distribution could be interpreted by exponentially distributed energy minima on a scale of 5–10 k_BT of the folded protein but does not preclude other scenarios. This result was surprising in that it points to a conformational diversity of proteins under force that is explored dynamically and may be important for protein function.

Here we directly measure the dwell time distribution of monomer proteins, where there is no uncertainty in N or averaging effects, and yet we reveal the same discrepancies from two-state behavior at the given force. Remarkably, the unfolding time distribution of the polyprotein directly overlaps with that of the monomer and spans over three decades, in support of both the Markovian hypothesis according to which the modules are independent of one another and the heterogeneous underlying distribution of unfolding pathways. The most striking result is shown by the agreement between the unfolding time distribution predicted in our previous work and that measured from the monomer data. Therefore, this new approach gives validity to the MLM in tackling polyprotein data, rules out effects of errors intrinsic to the method, suggests there are no correlations between the modules, and confirms the chain length independence of unfolding. Given this finding, one can now pool all the data together to extract the overall distribution, thus greatly simplifying the analysis. As a result, we find that the log normal distribution best describes the unfolding times, which is consistent with the power-law distribution of rates, predicted in our earlier work.

The force-clamp technique has also captured for the first time the folding trajectory of a single polyprotein. A two-pulse protocol first unfolds the protein at a high force and subsequently quenches it down to a lower force so as to trigger folding (33). The folding trajectories showed a number of distinct stages, involving both a force-dependent collapse of the extended polypeptide chain and the subsequent formation of the native contacts. Unlike the stochastic stepwise process observed for the unfolding, the folding appeared to be cooperative between the modules in the chain, which raised concerns as to the validity of the experiment. Whereas Sosnick attributed this cooperativity to an aggregation process between the neighboring domains within the polyprotein (12), Best and Hummer argued that the absence of steps was simply a result of entropic masking by the fluctuations of the unfolded polyprotein chain (15). Although the validity of these interpretations was strongly disputed (34,35), it is nonetheless difficult to decouple the individual modules in the folding trajectories, rendering their statistical analysis and interpretation difficult. Single-protein monomers bypass these issues because neither aggregation nor entropic masking can play a role. The use of AFM allows us to monitor the folding process of a single-protein module over a wider range of forces.

In this work, we first show that four different protein monomers can be distinguished from nonspecific interactions according to their characteristic step size given a sufficiently large pool of data. We then use the unfolding data to investigate the monomer unfolding rates for ubiquitin and I27 and find that the results agree with those obtained for the respective polyproteins. Next, we repeatedly refold both proteins and study the force-dependent folding kinetics for I27, which has never been probed under constant-force conditions. Pulling on individual monomers not only is a technical challenge but provides important insight into the protein-folding problem (36). Furthermore, experiments on monomers provide a closer comparison with bulk biochemistry experiments as well as with theoretical simulations involving both Go-models (37–39) and all-atom SMD simulations (40).

MATERIALS AND METHODS

Protein engineering

The polyproteins used in this study ($I27_8$ and $ProteinL_8$) were formed by consecutive subcloning of the respective monomers using the BamHI and

BglII restriction sites (1). The plasmid containing the B1 immunoglobulin binding domain of peptostreptococcal ProteinL (41) was a generous gift from Professor David Baker (University of Washington). The eight-domain I27 and the eight-domain ProteinL were cloned into the pQE80L (Qiagen) expression vector and transformed into the XL1 Blue *Escherichia coli* expression strain. This construct has two additional residues (arginine and serine) between each module in the chain. Constructs were purified by histidine metal-affinity chromatography with Talon resin (Clontech) and by gel filtration using a Superdex 200 HR column (GE Bio-Sciences). The same procedure was used for monomer engineering (I27, ubiquitin, and ProteinL), except for the multistep cloning step. All proteins used (monomers and polyproteins) are engineered with 12 extra residues in the C-terminus (MRGSHHHHHHGS-) and four extra residues in the N-terminus (-RSCC) that serve as ''handles'' in our experiments.

Force spectroscopy

Force-clamp atomic force microscopy experiments are conducted using a home-made setup under force-clamp conditions as described elsewhere (28,33). The sample is prepared by depositing 1–10 μl of protein in PBS solution (at a concentration of 1–10 μg ml^{-1} in the case of polyproteins, and ~10-fold higher concentration in the case of monomers) onto a freshly evaporated gold coverslide. The pickup ratio for the monomer proteins is, however, much lower than in the case of the respective polyproteins. Each cantilever (Si_3N_4 Veeco MLCT-AUHW) is individually calibrated using the equipartition theorem (42), giving rise to a typical spring constant of 20 pN nm^{-1}. Single proteins are picked up from the surface by pushing the cantilever onto the surface and exerting a contact force of 500–800 pN so as to promote the nonspecific adhesion of the proteins on the cantilever surface. The piezoelectric actuator is then retracted to produce a set deflection (force), which is constant throughout the experiment (~12–15 s) thanks to an external active feedback mechanism while the extension is recorded. The force feedback is based on a proportional, integral, and differential amplifier whose output is fed to the piezoelectric positioner. The feedback response is limited to ~3–5 ms. Because of the high-resolution piezoelectric actuator, our measurements of protein length have a peak-to-peak resolution of ~0.5 nm.

RESULTS AND DISCUSSION

Fingerprints of single unfolding events

Force-clamp traces of polyproteins yield staircases in which the height of each step corresponds to the number of amino acids released on unfolding a single module in the chain at a constant force. We can therefore distinguish between proteins by measuring their corresponding step height as the definitive molecular fingerprint, as shown in Fig. 1 for polyubiquitin (*A*), polyI27 (*C*), and polyProteinL (*E*). The accuracy of the technique allows us to detect small (~1 nm) differences in protein length, as exemplified by polyubiquitin (20.4 ± 0.7 nm @ 110 pN, $n = 244$, *B*), polyI27 (24.5 ± 0.5 nm @ 150 pN, $n = 188$, *D*), and polyproteinL (15.8 ± 0.9 nm @ 80 pN, $n = 456$, *F*). We then compare force-clamp data obtained

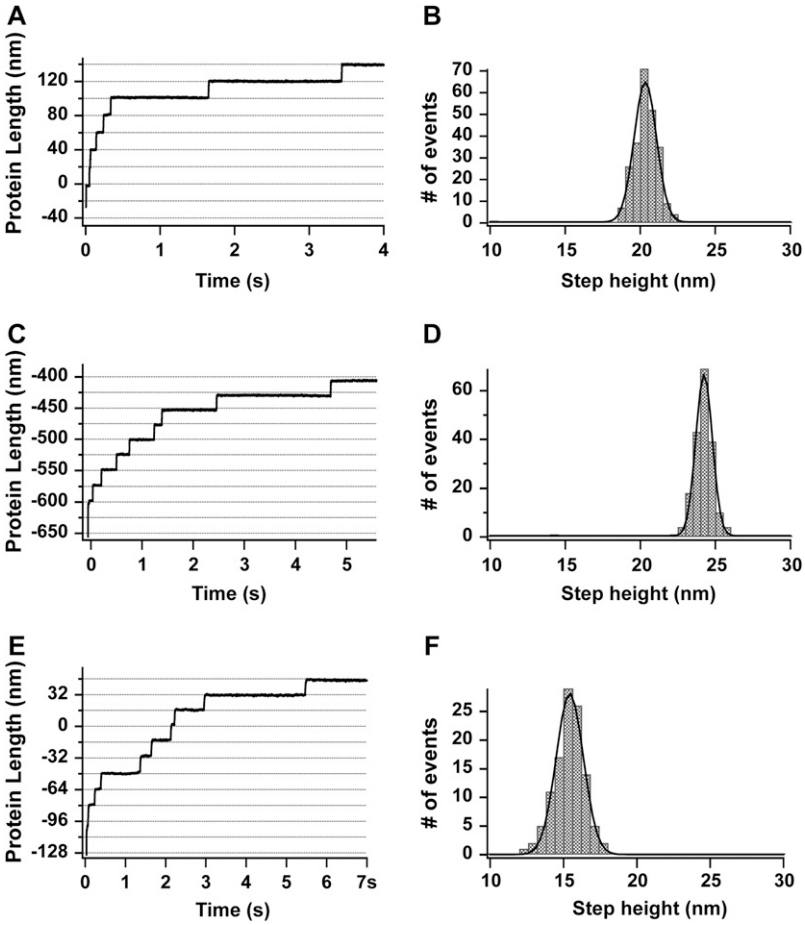

FIGURE 1 Typical length-versus-time recording of a concatamer of (*A*) Ubi_9, (*C*) $I27_8$, and (*E*) $PoteinL_8$ stretched at 110 pN, 150 pN, and 80 pN, respectively, yielding staircases in which every single step corresponds to the unfolding of a single module in the polyprotein chain. The measured step height is characteristic of each individual protein, thus serving as a fingerprint of the unfolded protein. Histograms of the measured step heights are shown for Ubi_9 pulled at 110 pN (*B*), $I27_8$ pulled at 150 pN (*D*), and $ProteinL_8$ pulled at 80 pN (*F*). Gaussian fits to the histograms give rise to step heights of 20.4 ± 0.7 nm (Ubi_9), 24.5 ± 0.5 nm ($I27_8$), and 15.8 ± 0.9 nm ($ProteinL_8$).

from single ubiquitin and I27 monomers with these standard values established for the respective polyproteins.

The monomers are stretched between the cantilever tip and the surface using the same experimental procedure as that of the polyprotein (43), schematically shown in Fig. 2 *A*. Fig. 2 *B* shows five typical traces corresponding to the unfolding of ubiquitin (*red*) at a pulling force of 90 pN and I27 (*blue*) stretched at 150 pN. Note that the first small steps in Fig. 2 *B* correspond to the extension of the folded ubiquitin (3.8 nm) or I27 (4.5 nm) and the monomer ''handles'' engineered on either side of the protein to facilitate protein pickup. The handles account for a maximum of 6.4 nm after correction for the deflection of the cantilever. Fig. 2 *C* shows the histograms of this first step size for ubiquitin (*red*, $n = 101$) yielding 6.6 ± 3.5 nm and for I27 (*blue*, $n = 153$), yielding 7.4 ± 4.2 nm. These values correspond to the most likely extension one would obtain if the proteins were picked up at random positions along the amino acid chain of the handles. Although most of the trajectories include an initial step that corresponds to the extension of the folded protein and the engineered handles, a few trajectories show an initial step that is longer than expected, as shown in the histogram (Fig. 2 *C*). Such longer handles may be the result of additional protein fragments that stick to the cantilever tip and are stretched in series with the protein monomer. This effect is also observed in polyprotein experiments. Nonetheless, the presence of longer handles does not have a measurable effect on the unfolding kinetics.

In each trace shown in Fig. 2 *B*, the fingerprint of the monomer is a single well-defined unfolding step of ~20.0 nm (ubiquitin, *red traces*) or ~24.5 nm (I27, *blue traces*), as expected for the unfolding of a single domain in the respective polyproteins (Fig. 1). The fingerprint of a polyprotein ensures that the probability of observing spurious interactions arising between the cantilever tip and the surface is negligible, although in the case of the monomer this probability is higher. Moreover, the success rate (i.e., the probability of picking up a single monomer) is typically ~10% of that of the polyprotein, which can be only partially compensated by a higher concentration of monomer on the surface. Improving the pickup ratio may be achieved by adding longer handles to the protein or designing a covalent bond between the surface and the protein. As noted before, a protein is likely to be picked up by the AFM tip forming an angle with the surface (Fig. 2 *A* (43)). Hence, it is also likely that the actual force applied to the molecule is slightly higher than the force measured from the vertical deflection of the cantilever. To get a rough estimate of this error, we consider that a stretched (but folded) single protein and its handles will form an angle with the pulling force. We assume a relaxed length for the folded protein on the surface of ~4.5 nm (I27 monomer). After pickup, the folded protein and its

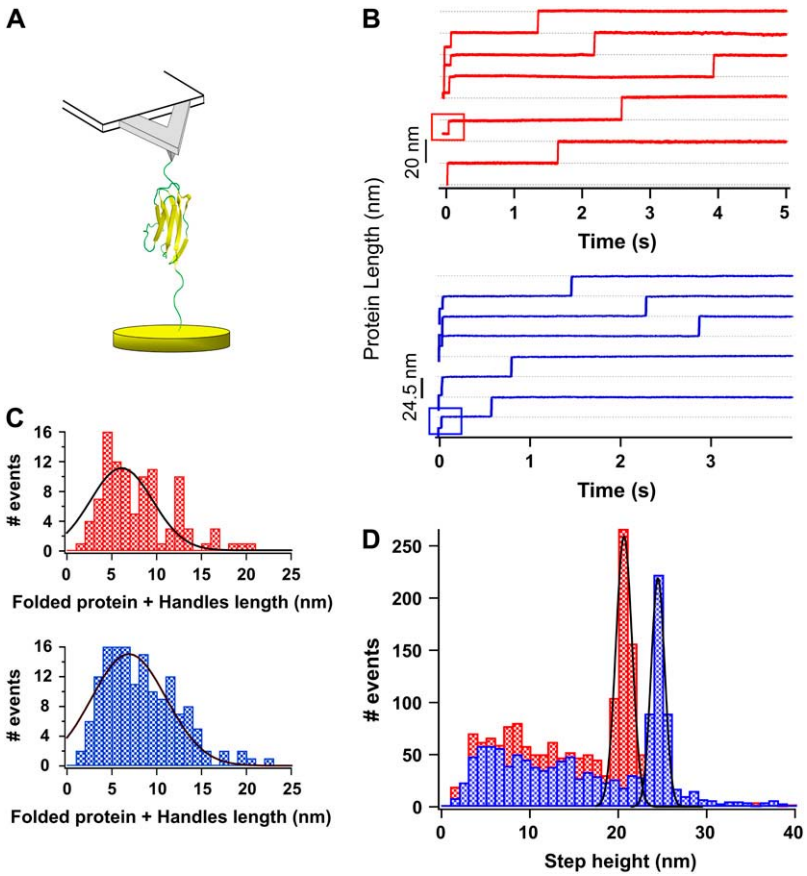

FIGURE 2 Single-protein monomers can be unambiguously unfolded with force-clamp spectroscopy. (*A*) Scheme of the experimental setup, where the single-protein monomer is held between the cantilever tip and the surface. (*B*) Five experimental length-versus-time recordings of ubiquitin monomers (*red traces*) stretched at 110 pN and of I27 monomers (*blue traces*) stretched at 150 pN, exhibiting well-defined steps at ~20.0 nm and ~24.5 nm, respectively. In all curves, an initial step before the unfolding step is observed (*red and blue squares*), described in the text. From this step size, the length of the folded protein with the handles can be measured for every particular trace, as shown in the histograms in *C*, (*ubiquitin, red; I27, blue*), which agrees with a random probability of pickup along the handles. (*D*) Histogram corresponding to all the recorded extensions for ubiquitin (*red; n* =1631) and I27 (*blue; n* =1317). Gaussian fit to the peaks in both histograms give rise to 20.65 ± 0.91 nm (ubiquitin) and 24.50 ± 0.77 nm (I27), as in the polyproteins (Fig. 1).

handles are stretched to a length of ~11 nm (4.5 nm of the folded protein plus the fully extended length of the handles) and form an angle of ~24° with the pulling force (worst case). Ignoring the effects of the asymmetry of the spring constant of the cantilever in different directions, we estimate that such a configuration would increase the pulling force by ~9%. The actual pulling angle will undoubtedly vary from molecule to molecule with an error varying in the range from 0% (the molecule is picked up and pulled straight up) and up to 9%.

To test the degree of confidence in the obtained results, we have plotted in Fig. 2 *D* a histogram of heights of all the 1631 steps measured for ubiquitin (*red bars*) and the 1317 steps measured for I27 monomers (*blue bars*). Both histograms show a well-defined peak and a flat background corresponding to steps of different heights that can be attributed to random nonspecific interactions between the tip and the sample. From the histograms, the nonspecific interactions that may be misinterpreted as unfolding events amount to ~22% of the area under the peak for ubiquitin and ~14% for that of I27. Because the distribution of nonspecific interactions is skewed toward smaller lengths, longer proteins have a higher level of confidence. Gaussian fits to each peak give rise to step heights of 20.7 ± 0.9 nm for ubiquitin and 24.5 ± 0.8 nm for I27, which are used in the subsequent analysis. Note the consistency of these results with the step height values measured for the polyproteins (Fig. 1).

To further prove the reliability of the technique, we present examples of monomeric unfolding events with ProteinL (Fig. 3) (44), with a stepsize of ~16 nm, in good agreement with the values obtained from the polyprotein (Fig. 1). Furthermore, we successfully unfold the monomer of a disulfide bonded I27 mutant up to the mechanically rigid disulfide bond, in a step of ~10.5 nm ($n = 329$), as shown in Fig. 4 *A* (45). When the same experiment is repeated in a reducing environment (50 mM DTT), the solvent-exposed disulfide bond can be reduced, thereby releasing the length of the molecule corresponding to the sequestered amino acids, which results in a second step of ~13.8 nm. (45). All these results show that experiments using monomer proteins are feasible, but we also point to the special attention that should be given to the contribution of spurious interactions with the surface, in particular for shorter proteins.

Unfolding kinetics

Using the acquired data, we studied the distribution of dwell times in the unfolding events to test whether the two-state kinetic model applies to the monomer data and whether the unfolding rates are exponentially dependent on the pulling force (28). Agreement with the polyprotein would help rule out possible artifacts, particularly those related to the contribution of nonspecific interactions and protein-surface tethering effects (38,46), which should be minimized by the presence of the engineered handles.

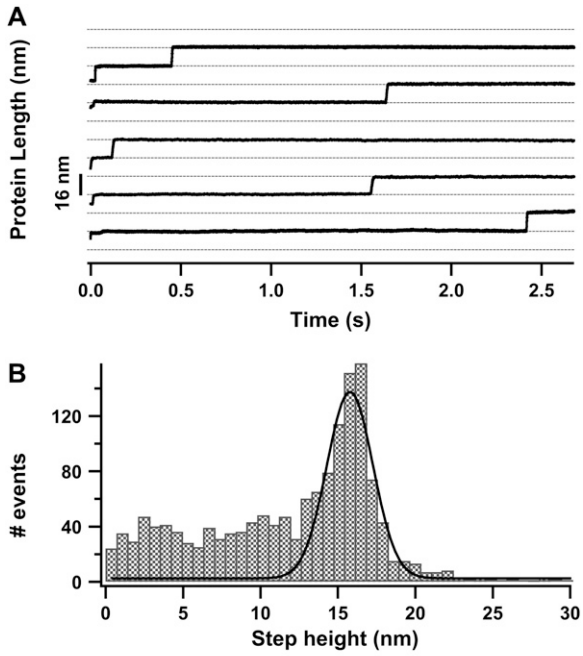

FIGURE 3 (*A*) Typical length-versus-time recordings corresponding to the unfolding of a ProteinL monomer when pulled at 80 pN, yielding a unique step with a measured step height of ~16 nm (*discontinuous lines* are to guide the eye). (*B*) Histogram corresponding to all the measured variations in length during four individual experiments at stretching forces ranging from 40 to 100 pN ($n = 1499$). Gaussian fit to the histogram peak yields a mean step height of 15.3 ± 2.16 nm.

In Fig. 5 *A* we show the unfolding probability of ubiquitin monomer at a constant force of 110 pN. When all the trajectories are included ($n = 343$, *red continuous line*), a single exponential fit (*red dashed line*) to the unfolding probability gives rise to an unfolding constant of $\alpha = 1.53\ s^{-1}$. However, in a typical force-clamp experiment, the proteins detach either from the cantilever or from the surface, such that the observed unfolding time distributions are biased to faster times. Selecting only those trajectories with detachment times greater than 1.5 s (*blue line*), we obtain a slower unfolding rate constant of $\alpha = 0.9\ s^{-1}$ (*gray dashed line*). Doubling the minimum detachment time to 3 s recovers the same unfolding probability (*green line*), showing that the effect of detachment time is negligible above 1.5 s at this force. This selection criterion greatly reduces the statistics of the experiment and is highly dependent on the force. For this reason, we unbias the unfolding time distribution by the detachment time distribution for each force by the following equation:

$$p(t_u) = \frac{p(t_u \cap t_d)}{\sum_{t_u}^{\infty} p(t_d|t_u)}, \quad (1)$$

where $p(t_u)$ is the true unfolding time distribution, $p(t_u \cap t_d)$ is the experimental probability distribution of unfolding times observed when the detachment time is larger than the

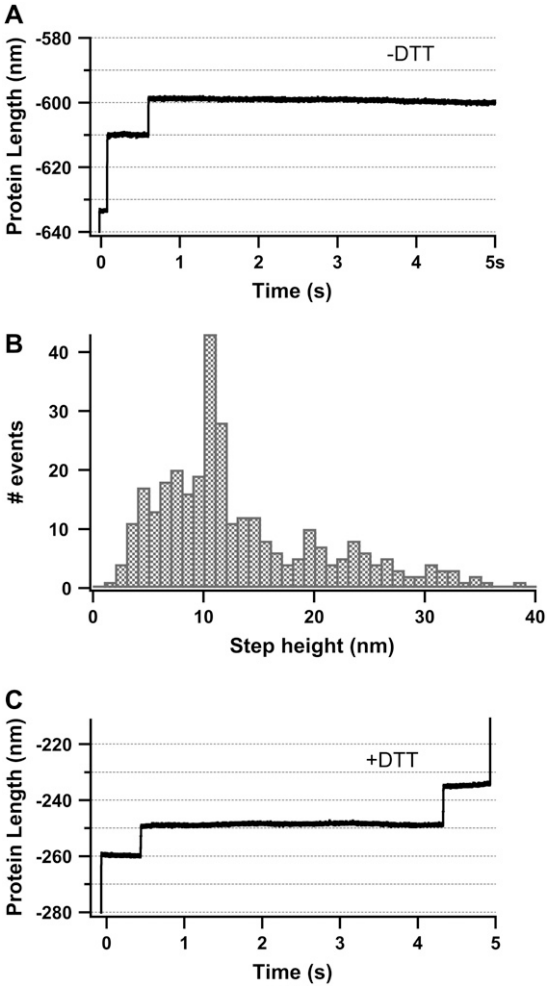

FIGURE 4 Chemical reactions can be monitored with single-protein monomers. (*A*) Typical length-versus-time recording showing the unfolding of a single $I27_{G32C\text{-}A75C}$ monomer stretched at 130 pN as confirmed by the presence of a unique ~10.5-nm step. (*B*) Histogram of all the measured step sizes ($n = 329$), which shows a preferential peak centered at ~10.5 nm. When the same experiment is repeated in a reducing environment (50 mM DTT), the length-versus-time traces exhibit two steps (*C*), the first one (~10.5 nm) corresponding to the unfolding of the $I27_{G32C\text{-}A75C}$ monomer, and the second one (~13.8 nm) corresponding to the reduction of the solvent-exposed disulfide bond, therefore releasing the previously sequestered amino acids.

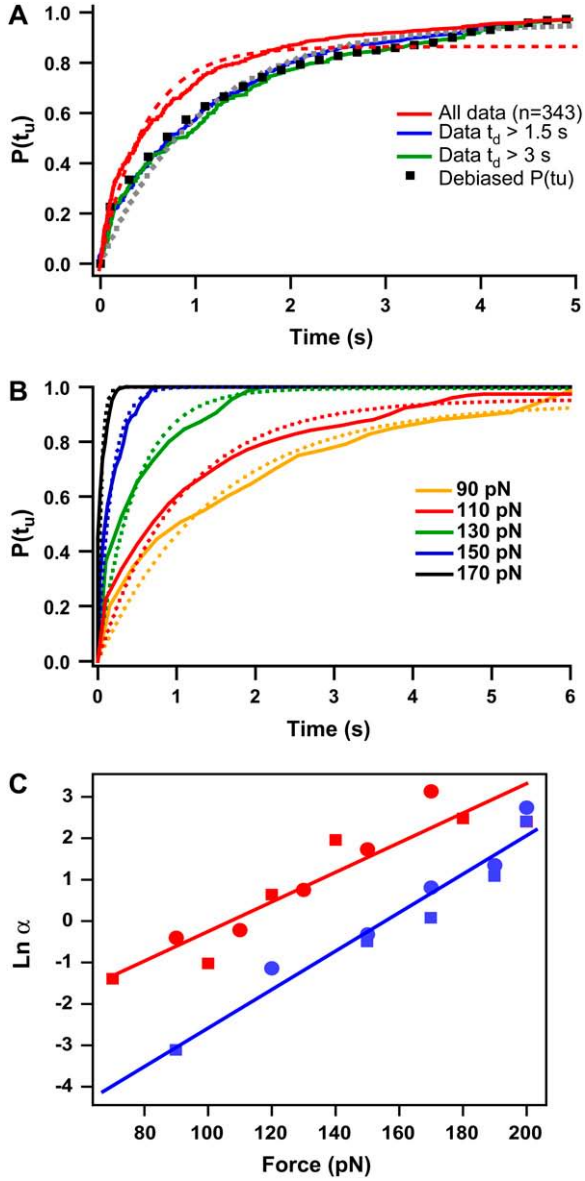

FIGURE 5 Unfolding kinetics for I27 and ubiquitin monomers present a close agreement with polyprotein data. (*A*) Unfolding probability of ubiquitin monomer at 110 pN. When all trajectories ($n = 343$) are included (*red line*), a single exponential fit (not constrained to 1, *dashed red line*) to the unfolding probability gives $\alpha = 1.53\ s^{-1}$. The fit (*gray dashed line*) to the unfolding probability of the trajectories with detachment time greater than 1.5 s (*blue line*) and 3 s (*green line*) gives $\alpha = 0.9\ s^{-1}$. Black squares show the cumulative probability of unfolding $P(t_u)$ obtained from unbiasing all the experimental data (*red line*) from their experimental detachment rate distribution according to Eq. 1 in the text. A single exponential fit to this curve yields $\alpha = 0.9\ s^{-1}$. (*B*) $P(t_u)$ distribution for ubiquitin monomer unfolding at 90, 110, 130, 150, and 170 pN. Distributions at each force are fitted to a single exponential curve (*dashed lines*) yielding the rate of unfolding at each particular force in a two-state model. (*C*) Plot of the logarithm of the rate constant as a function of the pulling force for ubiquitin (*red*) and I27 (*blue*). In both cases, circles stand for polyproteins and squares for the respective monomers. Data for polyubiquitin rates are extracted from Schlierf et al. (28). PolyI27 rates are obtained as shown in Fig. 7. Linear fit of Eq. 2 in the text to ubiquitin data (*red continuous line*) yields $\alpha_0 = 1.5 \times 10^{-2}\ s^{-1}$ and $\Delta x = 0.16$ nm and to I27 data (*blue continuous line*) yields $\alpha_0 = 7.2 \times 10^{-4}\ s^{-1}$ and $\Delta x = 0.19$ nm.

unfolding time, and $p(t_d|t_u)$is the experimental distribution of detachment times measured, given that the unfolding event has already occurred. Because we know the overall probability of detachment, we can then weight the experimentally observed unfolding time distribution by dividing by the fraction of events that detach after each unfolding time. We therefore account for the events that are not being observed. This unbiasing method is validated first using Monte Carlo simulations as shown in Fig. 6, assuming that both the unfolding time and the detachment time distributions follow first-order kinetics with rates approximated from the experimental data. The fact that the original distribution

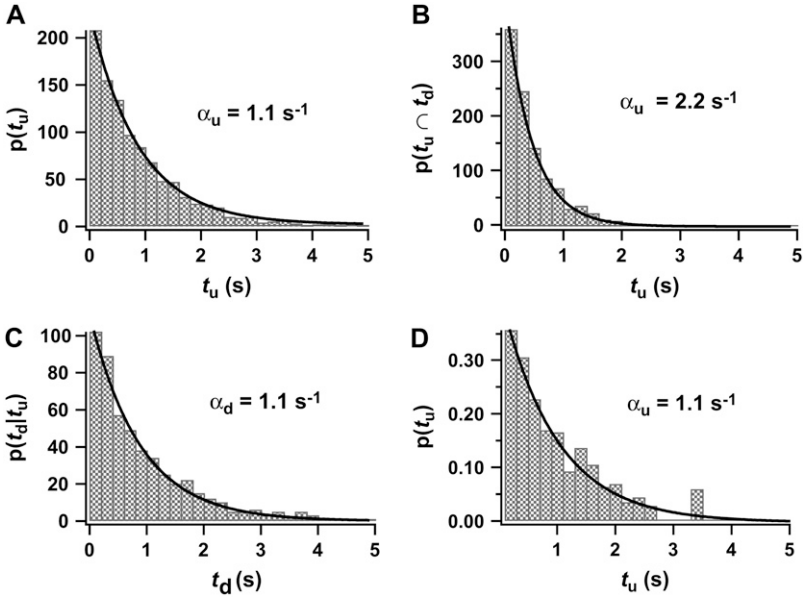

FIGURE 6 Monte-Carlo simulations validate the method for unbiasing the unfolding and the detachment rate distributions. (*A*) $p(t_u)$ distribution corresponding to 1000 independent simulations of ubiquitin monomer pulled at 110 pN assuming a two-state unfolding process without any effect of the detachment rate, giving rise to an unfolding constant $\alpha = 1.1\ s^{-1}$. (*B*) $p(t_u \cap t_d)$ distribution corresponding to 1000 independent simulations of ubiquitin monomer pulled at 110 pN with the effect of an exponentially distributed detachment rate of $\alpha_d = 1.1\ s^{-1}$ (distribution shown in *C*). Only in 511 of the 1000 attempts was the unfolding event measured, resulting in a ''biased'' unfolding constant $\alpha = 2.2\ s^{-1}$. (*D*) $p(t_u)$ distribution corresponding to unbiasing the $p(t_u \cap t_d)$ distribution shown in *B* by the associated detachment time distribution $p(t_d|t_u)$ shown in *C* by using Eq. 1 in the text. The resulting $p(t_u)$ distribution follows an unfolding kinetics with $\alpha = 1.1\ s^{-1}$, thus recovering the unfolding rate obtained in *A* when no effect of the detachment time was present.

is recovered gives confidence in the method. We then investigate the success of debiasing on the experimental data.

Black squares in Fig. 5 *A* show the integral of the probability density $p(t_u)$, which is the cumulative probability of unfolding as a function of time, $P(t_u)$. This distribution includes all the data and agrees with the cumulative probability of data selected for long detachment times, further validating the unbiasing method. In Fig. 5 *B*, we show $P(t_u)$ of ubiquitin for all the stretching forces spanning from 90 to 170 pN. At each force, $P(t_u)$ is fitted with a single exponential curve (*dashed lines*) according to the two-state model for unfolding, which was previously applied to the polyprotein data. Although the single exponential fits mostly reproduce the experimental data, deviations from the fit are already evident across the force range, which we discuss below.

The force dependence of the rate of unfolding has been shown in a previous work (28) to follow the Bell model

$$\alpha(F) = \alpha_0 \exp(F\Delta x/kT), \qquad (2)$$

where F is the pulling force, α_0 is the rate constant in the absence of force, and Δx is the distance to the transition state. The logarithm of the rate constant obtained for ubiquitin (Fig. 5 *B*) and I27 (data not shown) is plotted against the pulling force, giving rise to the trends shown in Fig. 5 *C*. In the case of both proteins, the monomer and polyprotein rate constants give rise to the same force dependence, as seen from the lines of best fit in red for ubiquitin and blue for I27. The unfolding rates for polyubiqutin are obtained from Schlierf et al. (28). Note that the unfolding rates of the I27 polyprotein are determined as shown in Fig. 7. Although the distance to the transition state is very similar for both proteins ($\Delta x = 0.16$ nm for ubiquitin and $\Delta x = 0.19$ nm for I27), their extrapolated unfolding rates in the absence of force are very different, with $\alpha_0 = 1.5 \times 10^{-2}\ s^{-1}$ for ubiquitin and $\alpha_0 = 7.2 \times 10^{-4}\ s^{-1}$ for I27. The monomer and polyprotein equivalence further reduces the contribution of protein-surface interactions to the data and proves the Markovian hypothesis. Furthermore, this result gives support to chemical denaturation experiments in the case of polyI27 (6), where the authors show the absence of domain-domain interactions. Interestingly, the measured Δx in the force-clamp mode is shorter than the values obtained in the force-extension mode with $\Delta x = 0.25$ nm for both molecules (1,21,28). Therefore, these results are consistent with a two-state unfolding picture in which as a first approximation the Bell model captures the unfolding force dependence and the most likely unfolding constant. Nonetheless, deviations from the single exponential fits to the data in Fig. 5 *A* invite an alternative physical model, in line with the previously developed analysis for polyubiquitin (31), which we investigate below.

In Fig. 8 we show that using a large pool of data ($n = 343$) at a constant force of 110 pN for ubiquitin monomer, the logarithmic binning of $p(t_u)$ reveals a broad distribution of

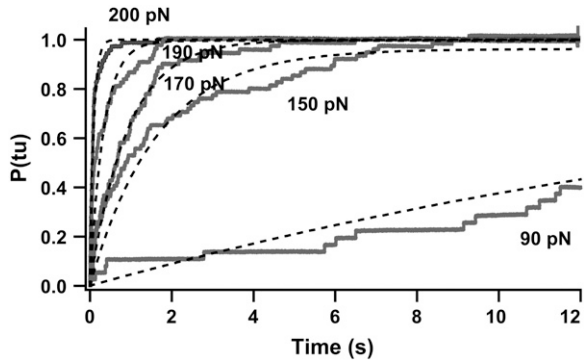

FIGURE 7 Five averaged and normalized polyI27 unfolding time courses obtained at different stretching forces: 90 pN, 150 pN, 170 pN, 190 pN, and 200 pN. Discontinuous black lines correspond to single exponential fits with rate constants presented as blue squares in Fig. 5 *C* in the text.

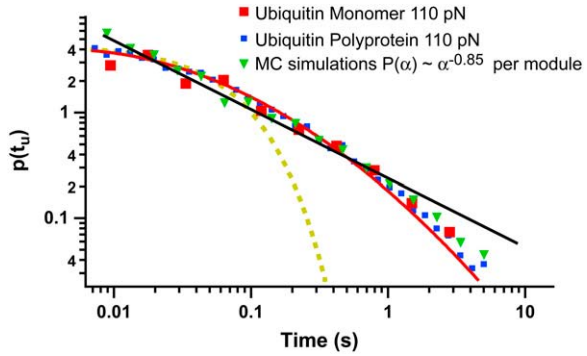

FIGURE 8 $p(t_u)$ of ubiquitin monomer (*red squares*) and polyprotein (*blue squares*) after logarithmic binning. The distribution of unfolding times is fitted to a log normal distribution (*solid red line*) and to a power law (*solid black line*), both deviating from the single exponential fit (*yellow dashed line*). Green triangles stand for the generated $p(t_u)$ that corresponds to the predicted $P(\alpha) \approx t^{-0.85}$ for a single monomer in Monte Carlo simulations (31). All the distributions are normalized by the area under the curve.

unfolding times spanning over three decades, which clearly cannot be captured by a single exponential fit (*yellow dashed curve*). Instead, the distribution is best fit with a log normal distribution, $p(t_u) \approx \exp(\ln(t/t_0)/\sigma)^2$, where $t_0 = 5$ ms and $\sigma = 3.0$ (*continuous red line*), or a power law, $p(t_u) \approx t^{-\gamma}$, with a decay coefficient $\gamma = 0.6$ in the range of times between 5 ms and 1 s (*continuous black line*). Because the polyprotein data were previously shown to be independent of both the number of modules in the chain, N, and the order number of the event in the chain, k, here we pool all the polyprotein unfolding dwell times together (corrected for the detachment time in the same way as the monomer data) for comparison. The overlap between the monomer (343 events) and the polyprotein data (4894 events) is remarkable, despite the significant portion of putative nonspecific events encountered by the monomer experiments in Fig. 2 *D*. It is unlikely that all the spurious events accumulate in the tail of the distribution because there is no evidence that nonspecific interactions should occur at long times. The observed agreement therefore indicates that the nonexponential behavior of proteins holds because of heterogeneity in the ensemble of native states; however, a contribution from artifacts cannot be entirely ruled out.

To compare with our previous results (31), using Monte Carlo simulations we generate a distribution of unfolding times (t_u) from the previously predicted power law distributed rates of $P(\alpha) \approx \alpha^{-0.85}$, each of which unfolds over a single barrier described by Eq. 2. We use the values of Δx and α_0 obtained from the fits in Fig. 5 *C* to generate 1000 unfolding times. The agreement between the resulting distribution and the experimental data is excellent. All the distributions are normalized by the area under the curve for comparison. Interestingly, distributions with slightly higher and lower power law decay coefficients (1.0 and 0.6, respectively) already start to deviate from the experimental distribution (data not shown), highlighting the accuracy of the MLM used with polyproteins (31). This result, which simply measures the distribution of unfolding times for monomers corrected for the effect of detachment rate using Eq. 1, is consistent with a rough energy landscape of the folded protein, in which the protein unfolds over multiple barriers with very different rates (32).

Capture of individual folding trajectories

The folding pathways explored by a single protein under force are different from those sampled in chemical and thermal bulk denaturation experiments (47) because they start from very different initial conditions and follow very different reaction coordinates. With the AFM, the high resolution in the end-to-end distance measurement allows us to map individual trajectories with subnanometer resolution during the entire refolding pathway (33).

Fig. 9 demonstrates the feasibility of folding single-protein monomers under a constant force. The experimental protocol in the case of the monomer proteins is the same as that of the polyproteins (33). The molecule is first stretched at a high force to unfold and subsequently quenched down to a lower force to trigger folding. To prove that the protein has indeed reformed its native contacts, the force is increased again to unfold the same monomer. In contrast to the polyproteins, here there is no ambiguity as to which module has folded. We first investigate the folding trajectories for I27 monomers as a function of the quenching force. Fig. 9 *A* shows three examples of cycles of unfolding and refolding of I27 monomers. In each case, we first observe a step of a length corresponding to the extension of the folded protein plus its handles (see Fig. 2 *C* and discussion in the text), followed by the well-defined 24.5-nm step corresponding to the unfolding of the I27 monomer. After 4 s, the pulling force was quenched down to 10 pN, 15 pN, and 20 pN, respectively. The protein is observed to collapse to different extents depending on the quenched force, as shown before in the case of ubiquitin polyproteins (33). Quenching the force to 10 pN typically leads to a very rapid collapse of the protein down to its folded length. An increase to 15 pN prolongs the folding time (~0.8 s in the second trace), resulting in a more complex collapse trajectory. Quenching to a higher force of 20 pN significantly increases the collapse time (~2.2 s, *third trace*) and leads to frequent failures where no folding is observed (*bottom trace*). Hence, on average, the higher the quenching force, the longer the folding time, τ_F, defined as the time at which the trajectories reach the baseline (folded length), as illustrated in the figure. It should be noted that we observe a broad range of collapse times to the folded length, even at a constant force, because of the rough energy landscape underlying the folding process. In all these traces, after the protein has been allowed to collapse and fold, the pulling force is increased again to unfold the refolded protein. This second pulse tests whether the protein had actually refolded by demonstrating that it had recovered its mechanical resistance.

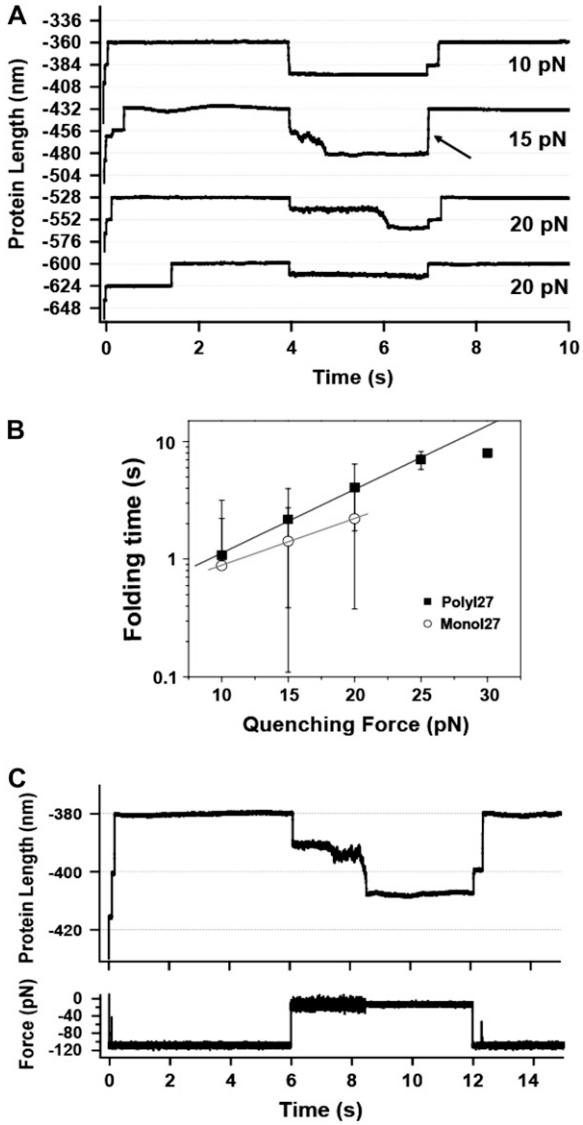

FIGURE 9 Folding times of single I27 monomers depend on the quenching force. (*A*) Experimental folding trajectories of the I27 monomer. In all cases, a two-pulse procedure has been used. The monomer is stretched at 120 pN for 4 s to unfold the protein, as revealed by the ~24.5-nm step (fingerprint of I27 unfolding) after the initial elastic elongation step (see Fig. 2 *C*). Subsequently, the force is quenched to a lower force (10 pN, 15 pN, or 20 pN) to trigger folding for 3 s. Finally, the force is again increased to 120 pN to unfold the monomer for another 3 s. In the upper trajectory the quenching force was set to 10 pN, and the folding process was almost instantaneous, thus showing an apparent two-state behavior. When the quenching force was set to 15 pN, the folding time was increased to ~0.8 s, thus resulting in a more complex folding trajectory. Finally, when the quenching force was set to 20 pN, the folding time increased to ~2.2 s or no folding was observed (failure trajectory). After the collapse takes place, the protein is stretched at higher force to promote the monomer reunfolding, marked by the steplike increase in length of ~24.5 nm. In the second trajectory (15 pN), the step occurs very fast, as shown by an arrow. (*B*) Logarithmic plot of the folding time, τ, as a function of the quenching force, for the polyprotein (*black squares*) and the monomer (*white circles*) I27. Data were fitted to an exponential relationship, yielding $\tau_F = 0.52 \exp(F \times 0.1)$ for the polyI27 (*black solid line*) and $\tau_F = 0.35 \exp(F \times 0.09)$ for the I27 monomer (*gray solid line*). (*C*) Typical force quench trajectory of ubiquitin. The monomer is pulled at 110 pN, and once it unfolds, the force is quenched down to 15 pN for 6 s. Within this period of time, the protein exhibits a contraction in length that leads to the folded length. Subsequently, the force is raised again to 110 pN to reunfold the monomer. The unfolding events can be easily identified in the force trace as ''spikes'' corresponding to the force feedback time.

On application of the second pulse, the folded protein and its handles extend first, resulting in a small step that in most cases is clearly visible and occurs exactly at the time of the force increase. This small step is followed, after a variable time, by the unfolding of the refolded I27 module, easily recognized as a 24.5-nm-long step that brings the protein back to its fully unfolded length (Fig. 9 *A*). In all cases the dwell time of unfolding is stochastically distributed. In the case of the trace where the pulling force was quenched to 15 pN (*second trace*), the 24.5-nm unfolding step occurred almost immediately after the application of the second pulse, making it difficult to separate from the extension of the folded protein. These can be observed as separate steps (marked by the *arrow* in Fig. 9 *A*) on a faster timescale.

The distribution of folding times from all the folding data of monomer I27 ($n = 66$) can be fitted to an exponential relationship between the folding times and the quenching force,

$$\tau_F = 0.35 \exp(F \times 0.09), \quad (3)$$

presented in Fig. 9 *B*. For comparison, we also present new folding data for polyI27 in Fig. 10, showing that modules contract to the folded length cooperatively, as previously reported in the case of polyubiquitin (35). The average folding times for all such trajectories reveal the collapse time dependence on the force for polyprotein I27 ($n = 102$), yielding $\tau_F = 0.52$ exp ($F \times 0.1$). The results are in good agreement with the monomer data, although it should be noted that the monomers fold faster on average. This is consistent with the observation that longer polyprotein chains collapse to the folded length more slowly than shorter ones, as shown elsewhere (33). Interestingly, the folding times in the absence of force for polyI27 and monoI27 give rise to folding rates of $1/\tau_{0,F} = 1.92\ s^{-1}$ and $2.86\ s^{-1}$, respectively, which is in close agreement with the value measured from force-extension measurements for polyI27, $1/\tau_{0,F} = 1.2\ s^{-1}$ (1).

The force-clamp experiment on I27 single domains has been recently performed in silico (37). In this work, Thirumalai and co-workers pointed out the importance of initial conditions before quenching the force on the resulting trajectories, inducing a multiplicity of folding pathways in their Go-model simulations, which may explain the broad distribution of folding times we observe experimentally. The collapse times also obey an exponential relationship in their numerical simulations.

For comparison, we show a full trajectory of ubiquitin as a function of both force and length in Fig. 9 *C*, which follows the unfolding and refolding processes. The folding trajectories

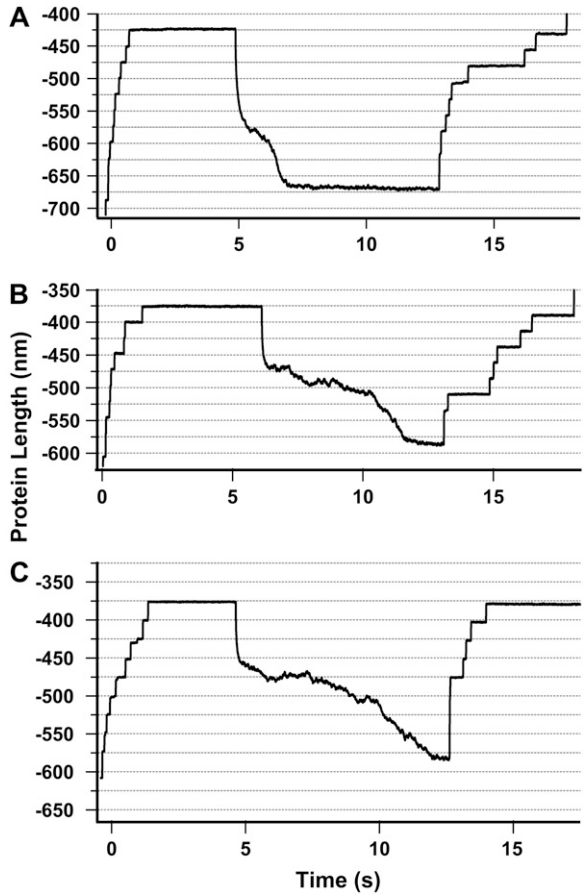

FIGURE 10 (*A*) Three typical folding trajectories of an $I27_8$ polyprotein. The polyprotein was unfolded at high force (150 pN) as confirmed by the stepwise ~24.5-nm increment in length. Then, the force is quenched down to (*A*) 15 pN, (*B*) 20 pN, or (*C*) 25 pN so as to favor folding. As has been previously described for polyubiquitin (33), folding trajectories, unlike unfolding ones, occur cooperatively and feature large fluctuations in length during the pathway that leads the protein from the unfolded state to the folded state. Therefore, the general folding trends observed for polyubiquitin trajectories also apply to polyI27. Note that, on average, the lower the quenching force, the higher the time the molecule needs to fold (*A–C*).

of monomer ubiquitin ($n = 12$) and I27 ($n = 66$) exhibit the same stages in folding. We observe a rapid contraction from entropic recoil down to an average length of 83% of the contour length, followed by a diffusive search of the highly extended conformational states and, finally, a fast collapse all the way down to the folded state length. In the case of ubiquitin, the final contraction to the folded length is ~14 nm, which is in good agreement with the value found for the polyprotein trajectories rescaled by the number of modules present in the chain (35). By contrast, I27 exhibits an even longer average contraction of 23 nm, attributable to its 4 nm longer contour length. Note that the end-to-end length fluctuations increase over time, both in the length trace and also in the force trace along the folding trajectory (Fig. 9 *C*), because the cantilever and the molecule are mechanically coupled (48). The monomer trajectories, which do not suffer from entropic masking or aggregation, therefore give validity to those of the polyprotein and highlight the physical features of folding that arise when a protein is extended far from its native configuration.

In summary, we have shown that force spectroscopy experiments can be performed at the monomer level, resolving many of the issues presented in the literature. First, they exclude the possibility of protein-protein interactions while reproducing the kinetics of unfolding of polyproteins. This is a strong indication that these interactions do not affect polyprotein data, where the events are indeed Markovian. The average unfolding rate constant (i.e., the barrier height) is exponentially dependent on the applied force and gives a useful approximation for the fragility of the protein. A statistical analysis with a larger statistical pool of data reveals that ubiquitin monomers exhibit a broad distribution of unfolding times at 110 pN, which are best described by a log normal distribution. This result is consistent with the power-law distribution of times measured for the polyprotein and reminiscent of a complex energy landscape with multiple traps exhibiting energy minima on a scale of 5–10 k_BT. Moreover, the monomer data reveal the folding pathways that are not affected by the presence of neighboring domains, simplifying their interpretation. In particular, the fluctuations are faithful to the exploration of the protein landscape far from the folded state as well as the driving forces responsible for the rapid contraction toward the folded state. These can now be investigated at the molecular level, also by computer simulations.

We thank Professor David Baker (University of Washington) for his generous gift of the plasmid containing the sequence of the B1 domain of ProteinL. We are indebted to Andrew J. Tolley and Jean-Philippe Bouchaud for useful comments. We thank Rodolfo I. Hermans Z. for helpful discussions and assistance in programming, Dr. Raul Perez-Jimenez and other members of the J.M.F. Laboratory for discussions. S.G.-M. thanks the Generalitat de Catalunya for a postdoctoral fellowship through the NANO and Beatriu de Pinós programs. J.B. holds a Career Award at the Scientific Interface from the Burroughs Wellcome Fund. This work was supported by NIH Grants HL66030 and HL61228 (to J.M.F).

REFERENCES

1. Carrion-Vazquez, M., A. Oberhauser, S. Fowler, P. Marszalek, S. Broedel, J. Clarke, and J. Fernandez. 1999. Mechanical and chemical unfolding of a single protein: a comparison. *Proc. Natl. Acad. Sci. USA*. 96:3694–3699.
2. Dietz, H., M. Bertz, M. Schlierf, F. Berkemeier, T. Bornschlogl, J. P. Junker, and M. Rief. 2006. Cysteine engineering of polyproteins for single-molecule force spectroscopy. *Nat. Protocols*. 1:80–84.
3. Dietz, H., F. Berkemeier, M. Bertz, and M. Rief. 2006. Anisotropic deformation response of single protein molecules. *Proc. Natl. Acad. Sci. USA*. 103:12724–12728.
4. Fernandez, J. M. 2005. Fingerprinting single molecules in vivo. *Biophys. J*. 89:3676–3677.
5. Rounsevell, R. W. S., A. Steward, and J. Clarke. 2005. Biophysical investigations of engineered polyproteins: implications for force data. *Biophys. J*. 88:2022–2029.

6. Scott, K. A., A. Steward, S. B. Fowler, and J. Clarke. 2002. Titin; a multidomain protein that behaves as the sum of its parts. *J. Mol. Biol.* 315:819–829.
7. Batey, S., K. A. Scott, and J. Clarke. 2006. Complex folding kinetics of a multidomain protein. *Biophys. J.* 90:2120–2130.
8. Law, R., P. Carl, S. Harper, P. Dalhaimer, D. Speicher, and D. Discher. 2003. Cooperativity in forced unfolding of tandem spectrin repeats. *Biophys. J.* 84:533–544.
9. Li, H., A. Oberhauser, S. Fowler, J. Clarke, and J. Fernandez. 2000. Atomic force microscopy reveals the mechanical design of a modular protein. *Proc. Natl. Acad. Sci. USA.* 97:6527–6531.
10. Wright, C. F., S. A. Teichmann, J. Clarke, and C. M. Dobson. 2005. The importance of sequence diversity in the aggregation and evolution of proteins. *Nature.* 438:878–881.
11. Carulla, N., G. L. Caddy, D. R. Hall, J. Zurdo, M. Gairi, M. Feliz, E. Giralt, C. V. Robinson, and C. M. Dobson. 2005. Molecular recycling within amyloid fibrils. *Nature.* 436:554–558.
12. Sosnick, T. R. 2004. Comment on ''Force-clamp spectroscopy monitors the folding trajectory of a single protein.'' *Science.* 306:411.
13. Rousseau, F., J. W. H. Schymkowitz, and L. S. Itzhaki. 2003. The unfolding story of three-dimensional domain swapping. *Structure.* 11:243–251.
14. Bryant, Z., M. D. Stone, J. Gore, S. B. Smith, N. R. Cozzarelli, and C. Bustamante. 2003. Structural transitions and elasticity from torque measurements on DNA. *Nature.* 424:338–341.
15. Best, R. B., and G. Hummer. 2005. Comment on ''Force-clamp spectroscopy monitors the folding trajectory of a single protein''. *Science.* 308:498.
16. Dietz, H., and M. Rief. 2004. Exploring the energy landscape of GFP by single-molecule mechanical experiments. *Proc. Natl. Acad. Sci. USA.* 101:16192–16197.
17. Schwaiger, I., M. Schleicher, A. A. Noegel, and M. Rief. 2005. The folding pathway of a fast-folding immunoglobulin domain revealed by single-molecule mechanical experiments. *EMBO Rep.* 6:46–51.
18. Perez-Jimenez, R., S. Garcia-Manyes, S. Rama Koti Ainavarapu, and J. M. Fernandez. 2006. Mechanical unfolding pathways of the enhanced yellow fluorescent protein (EYFP) revealed by single-molecule force spectroscopy. *J. Biol. Chem.* 281:40010–40014.
19. Sharma, D., Y. Cao, and H. B. Li. 2006. Engineering proteins with novel mechanical properties by recombination of protein fragments. *Angew. Chem. Int. Ed. Engl.* 45:5633–5638.
20. Rief, M., J. Fernandez, and H. Gaub. 1997. Reversible unfolding of individual titin immunoglobulin domains by AFM. *Science.* 276:1109–1112.
21. Carrion-Vazquez, M., H. Li, H. Lu, P. Marszalek, A. Oberhauser, and J. Fernandez. 2003. The mechanical stability of ubiquitin is linkage dependent. *Nat. Struct. Biol.* 10:738–743.
22. Oberhauser, A., P. Marszalek, H. Erickson, and J. Fernandez. 1998. The molecular elasticity of the extracellular matrix protein tenascin. *Nature.* 393:181–185.
23. Rief, M., J. Pascual, M. Saraste, and H. E. Gaub. 1999. Single molecule force spectroscopy of spectrin repeats: Low unfolding forces in helix bundles. *J. Mol. Biol.* 286:553–561.
24. Dugdale, T. M., R. Dagastine, A. Chiovitti, P. Mulvaney, and R. Wetherbee. 2005. Single adhesive nanofibers from a live diatom have the signature fingerprint of modular proteins. *Biophys. J.* 89:4252–4260.
25. Bullard, B., T. Garcia, V. Benes, M. C. Leake, W. A. Linke, and A. F. Oberhauser. 2006. The molecular elasticity of the insect flight muscle proteins projectin and kettin. *Proc. Natl. Acad. Sci. USA.* 103:4451–4456.
26. Cecconi, C., E. A. Shank, C. Bustamante, and S. Marqusee. 2005. Direct observation of the three-state folding of a single protein molecule. *Science.* 309:2057–2060.
27. Oberhauser, A., P. Hansma, M. Carrion-Vazquez, and J. Fernandez. 2001. Stepwise unfolding of titin under force-clamp atomic force microscopy. *Proc. Natl. Acad. Sci. USA.* 98:468–472.
28. Schlierf, M., H. Li, and J. Fernandez. 2004. The unfolding kinetics of ubiquitin captured with single-molecule force-clamp techniques. *Proc. Natl. Acad. Sci. USA.* 101:7299–7304.
29. Bell, G. I. 1978. Models for specific adhesion of cells to cells. *Science.* 200:618–627.
30. Brujic, J., R. I. Hermans, S. Garcia-Manyes, K. A. Walther, and J. M. Fernandez. 2007. Dwell-time distribution analysis of polyprotein unfolding using force-clamp spectroscopy. *Biophys. J.* 92:2896–2903.
31. Brujic, J., R. I. Hermans, K. A. Walther, and J. M. Fernandez. 2006. Single-molecule force spectroscopy reveals signatures of glassy dynamics in the energy landscape of ubiquitin. *Nature Physics.* 2:282–286.
32. Monthus, C., and J. P. Bouchaud. 1996. Models of traps and glass phenomenology. *J Phys a-Math Gen* 29:3847–3869.
33. Fernandez, J., and H. Li. 2004. Force-clamp spectroscopy monitors the folding trajectory of a single protein. *Science.* 303:1674–1678.
34. Fernandez, J., H. Li, and B. J. 2004. Response to comment on ''Force-clamp spectroscopy monitors the folding trajectory of a single protein.'' *Science.* 306:411c.
35. Brujic, J., and J. W. Fernandez. 2005. Response to comment on ''Force-clamp spectroscopy monitors the folding trajectory of a single protein.'' *Science.* 308:498.
36. Thirumalai, D. 1995. From minimal models to real proteins: time scales for protein folding kinetics. *J. Phys. I France.* 5:1457–1467.
37. Li, M. S., C. K. Hu, D. K. Klimov, and D. Thirumalai. 2006. Multiple stepwise refolding of immunoglobulin domain I27 upon force quench depends on initial conditions. *Proc. Natl. Acad. Sci. USA.* 103: 93–98.
38. Cieplak, M., and P. Szymczak. 2006. Protein folding in a force clamp. *J. Chem. Phys.* 124:194901.
39. Li, M. S., M. Kouza, and C.-K. Hu. 2006. Refolding upon force quench and pathways of mechanical and thermal unfolding of ubiquitin. *Biophys. J.* 92:547–561.
40. Grater, F., and H. Grubmuller. 2007. Fluctuations of primary ubiquitin folding intermediates in a force clamp. *J. Struct. Biol.* 157:557–569.
41. Kim, D. E., C. Fisher, and D. Baker. 2000. A breakdown of symmetry in the folding transition state of protein L. *J. Mol. Biol.* 298:971–984.
42. Florin, E. L., M. Rief, H. Lehmann, M. Ludwig, C. Dornmair, V. T. Moy, and H. E. Gaub. 1995. Sensing specific molecular-interactions with the atomic-force microscope. *Biosens. Bioelectron.* 10:895–901.
43. Carrion-Vazquez, M., P. E. Marszalek, A. F. Oberhauser, and J. M. Fernandez. 1999. Atomic force microscopy captures length phenotypes in single proteins. *Proc. Natl. Acad. Sci. USA.* 96:11288–11292.
44. Brockwell, D. J., G. S. Beddard, E. Paci, D. K. West, P. D. Olmsted, D. A. Smith, and S. E. Radford. 2005. Mechanically unfolding the small, topologically simple protein L. *Biophys. J.* 89:506–519.
45. Wiita, A. P., S. R. K. Ainavarapu, H. H. Huang, and J. M. Fernandez. 2006. Force-dependent chemical kinetics of disulfide bond reduction observed with single-molecule techniques. *Proc. Natl. Acad. Sci. USA.* 103:7222–7227.
46. Friedel, M., A. Baumketner, and J. E. Shea. 2006. Effects of surface tethering on protein folding mechanisms. *Proc. Natl. Acad. Sci. USA.* 103:8396–8401.
47. Zhuang, X. W., and M. Rief. 2003. Single-molecule folding. *Curr. Opin. Struct. Biol.* 13:88–97.
48. Walther, K. A., J. Brujic, H. B. Li, and J. M. Fernandez. 2006. Sub-angstrom conformational changes of a single molecule captured by AFM variance analysis. *Biophys. J.* 90:3806–3812.